

# Gd<sub>2</sub>O<sub>3</sub> nanoparticles in hematopoietic cells for MRI contrast enhancement

Anna Hedlund<sup>1,2</sup>Maria Åhrén<sup>3</sup>Håkan Gustafsson<sup>1,2</sup>Natalia Abrikosova<sup>3</sup>Marcel Warntjes<sup>2,4</sup>Jan-Ingvar Jönsson<sup>5</sup>Kajsa Uvdal<sup>3</sup>Maria Engström<sup>1,2</sup>

<sup>1</sup>Division of Radiology, Department of Medical and Health Sciences, <sup>2</sup>Center for Medical Image Science and Visualization, <sup>3</sup>Division of Molecular Surface Physics and Nanoscience, Department of Physics, Chemistry, and Biology, <sup>4</sup>Division of Clinical Physiology, Department of Medicine and Health Sciences, <sup>5</sup>Department of Clinical and Experimental Medicine, Experimental Hematology Unit, Linköping University, Linköping, Sweden

**Abstract:** As the utility of magnetic resonance imaging (MRI) broadens, the importance of having specific and efficient contrast agents increases and in recent time there has been a huge development in the fields of molecular imaging and intracellular markers. Previous studies have shown that gadolinium oxide (Gd<sub>2</sub>O<sub>3</sub>) nanoparticles generate higher relaxivity than currently available Gd chelates. In addition, the Gd<sub>2</sub>O<sub>3</sub> nanoparticles have promising properties for MRI cell tracking. The aim of the present work was to study cell labeling with Gd<sub>2</sub>O<sub>3</sub> nanoparticles in hematopoietic cells and to improve techniques for monitoring hematopoietic stem cell migration by MRI. Particle uptake was studied in two cell lines: the hematopoietic progenitor cell line Ba/F3 and the monocytic cell line THP-1. Cells were incubated with Gd<sub>2</sub>O<sub>3</sub> nanoparticles and it was investigated whether the transfection agent protamine sulfate increased the particle uptake. Treated cells were examined by electron microscopy and MRI, and analyzed for particle content by inductively coupled plasma sector field mass spectrometry. Results showed that particles were intracellular, however, sparsely in Ba/F3. The relaxation times were shortened with increasing particle concentration. Relaxivities,  $r_1$  and  $r_2$  at 1.5 T and 21°C, for Gd<sub>2</sub>O<sub>3</sub> nanoparticles in different cell samples were 3.6–5.3 s<sup>-1</sup> mM<sup>-1</sup> and 9.6–17.2 s<sup>-1</sup> mM<sup>-1</sup>, respectively. Protamine sulfate treatment increased the uptake in both Ba/F3 cells and THP-1 cells. However, the increased uptake did not increase the relaxation rate for THP-1 as for Ba/F3, probably due to aggregation and/or saturation effects. Viability of treated cells was not significantly decreased and thus, it was concluded that the use of Gd<sub>2</sub>O<sub>3</sub> nanoparticles is suitable for this type of cell labeling by means of detecting and monitoring hematopoietic cells. In conclusion, Gd<sub>2</sub>O<sub>3</sub> nanoparticles are a promising material to achieve positive intracellular MRI contrast; however, further particle development needs to be performed.

**Keywords:** gadolinium oxide, magnetic resonance imaging, contrast agent, cell labeling, Ba/F3 cells, THP-1 cells

## Introduction

Magnetic resonance imaging (MRI) is an important technique for medical image diagnostics. It has a unique ability to distinguish soft body tissue through endogenous contrast mechanisms. Exogenous contrast agents are frequently used in MRI for contrast enhancement and there are a variety of agents commercially available. Negative contrast is obtained by using superparamagnetic iron oxide particles. However, the most common clinically used substances, which give positive contrast enhancement, are paramagnetic chelates based on gadolinium (Gd) complexes. The Gd<sup>3+</sup> ion, with seven unpaired f-electrons, is a preferred substance for contrast enhancement in MRI due to its paramagnetic properties. Gd chelates are, however, not very selective

Correspondence: Maria Engström  
Center for Medical Image Science and Visualization/Department of Medical and Health Sciences, Linköping University/US, SE-581 85 Linköping, Sweden  
Tel +46 10 1038 901  
Email maria.engstrom@liu.se

and have low relaxivity compared to what is theoretically possible.<sup>1</sup> In addition, when using Gd chelates as contrast agents, relatively high doses could be required due to the widespread distribution. Administration to patients with reduced renal clearance is linked to nephrogenic systemic fibrosis.<sup>2–4</sup> Nephrogenic systemic fibrosis is a scleroma-like fibrotic skin disorder observed for patients with renal impairment. Deposits of collagen in tissues and skin are characteristic with skin thickening and hyperpigmentation as hallmarks. The disorder may have systemic involvement and in severe cases it can be fatal.<sup>5</sup> Therefore it is of importance that low doses of Gd are used without losing contrast effect, which drives the research of finding more efficient Gd-based agents. For this reason, Gd oxide ( $\text{Gd}_2\text{O}_3$ ) nanoparticles have gained attention.<sup>6–8</sup> In contrast to superparamagnetic iron oxide particles,  $\text{Gd}_2\text{O}_3$  can easily generate positive contrast, thereby avoiding loss of signal and image voids that generally occur when using susceptibility contrast agents. Such signal loss could make it difficult to detect the contrast agent and discriminate between the agent, tissue, and image artifacts.

In addition, the field of molecular imaging using MRI in conjunction with contrast agents is increasingly improving and different cell labeling contrast agents have been developed in recent years. For such cell labeling studies, the development of positive contrast agents like  $\text{Gd}_2\text{O}_3$  nanoparticles providing high signal per unit is of great interest.<sup>9</sup> MRI combined with molecular imaging will allow monitoring of specific tissues or cell types, for instance detection of stem cell migration and cellular trafficking, differentiation, and transplant rejection. Other available methods for cell visualization include genetic labels, radionuclides, or membrane dyes.<sup>10,11</sup> However, MRI is among the least invasive of the currently available imaging methods. It is considered safe and would thus be preferred as a tracking method.

It is recognized that particulate agents of iron oxide, coated with dextran for example, can be internalized into a variety of cell types and labeling efficacy can be increased using different transfection agents, especially for cell types that are not naturally phagocytic.<sup>12–14</sup> It has been shown earlier that THP-1 monocytes labeled with  $\text{Gd}_2\text{O}_3$  nanoparticles provide positive contrast in MRI.<sup>15</sup> In the current work, the aim was to continue this research by visualizing intracellular particles with electron microscopy and to explore whether a hematopoietic progenitor cell line, Ba/F3, would take up the particles or not, and if a transfection agent could further improve uptake in the Ba/F3 cells. MRI was used to assess whether high MRI contrast could be obtained from the  $\text{Gd}_2\text{O}_3$  nanoparticle-labeled cells. This study is part of a long term

goal to improve the possibilities to monitor, for instance, stem cell migration with MRI by taking advantage of the positive contrast rendered by  $\text{Gd}_2\text{O}_3$  nanoparticles.

## Materials and methods

### $\text{Gd}_2\text{O}_3$ nanoparticles

The polyol method<sup>16,17</sup> was used for synthesis of the  $\text{Gd}_2\text{O}_3$  particles.  $\text{GdCl}_3 \cdot 6\text{H}_2\text{O}$  (2 mmol) was dissolved in 10 mL diethylene glycol (DEG) by heating to 140°C. Solid sodium hydroxide (2.5 mmol) was dissolved in 10 mL DEG and subsequently added to the Gd-containing solution. The temperature was raised to 180°C and held constant for 4 hours under reflux and magnetic stirring, yielding a colloid. The solubility product or stability constant for  $\text{Gd}_2\text{O}_3$  ( $K_{\text{sp}} = [\text{Gd}^{3+}]^2[\text{OH}^-]^6$ ) is of the order  $\sim 10^{-31}$ , as calculated from thermodynamic data, hence the oxide is unstable in water at neutral pH.<sup>15</sup> However, the solubility kinetics is quite slow.

To exclude aggregates and ions, the particle solution was filtered and dialyzed. A Vivaspin® polyethersulfone filter (Sartorius Vivascience AG, Hanover, Germany) with pore size 0.2  $\mu\text{m}$  was used and filtering was performed by centrifuging the solution (1750 rpm) until all fluid had passed the filter (about 30 minutes). Then the samples were dialyzed in Milli-Q water (Millipore Corporation, Billerica, MA) using a membrane with a pore size of 1000 molecular weight cut-off. Dialysis proceeded for 24 hours and the water was changed three times. The sample-to-volume ratio in the dialysis procedure was at least 1:1000.

Particles were characterized through high-resolution transmission electron microscopy using a Tecnai™ G2 electron microscope (FEI Company, Hillsboro, OR) operated at 200 kV. X-ray photoelectron spectroscopy studies were performed using a Microlab 310F (Thermo VG Scientific, West Sussex, United Kingdom) with a hemispheric analyzer and unmonochromatized aluminum K $\alpha$  photons (1486.6 eV). The pressure in the analysis chamber was approximately  $2 \times 10^{-8}$  mbar and the resolution was determined from the full-width half-maximum of the gold ( $4f_{7/2}$ ) line, which was about 2 eV with pass energy 50 eV. Sample preparations for transmission electron microscopy and X-ray photoelectron spectroscopy are described in Klasson et al.<sup>15</sup>

### Cell culturing and labeling

A hematopoietic progenitor cell line, Ba/F3, was used in this study and compared to a monocytic cell line, THP-1. Ba/F3 is a murine pro B-cell line established from mouse fetal liver.<sup>18</sup> The cell line grows in suspension (Roswell Park Memorial Institute 1640 medium with 10% fetal bovine serum, 2 mM L-glutamine,

25 mM HEPES, 50  $\mu$ M 2-mercaptoethanol, 1% penicillin-streptomycin and 5% interleukin-3 [Sigma-Aldrich, St Louis, MO] and is kept in a cell culture flask at 37°C in 5% carbon dioxide atmosphere. As for the THP-1 cells, they are human monocytic cells derived from a 1-year-old boy with acute monocytic leukemia.<sup>19</sup> They are phagocytic and grow in suspension (Roswell Park Memorial Institute 1640 medium with 10% fetal bovine serum, 2 mM L-glutamine, 1% penicillin-streptomycin) with the same atmospheric conditions as for Ba/F3.

Experiments were conducted as follows; cells were transferred to 24-well culturing plates and each sample contained one million cells in 1 mL of cell culture medium. Cells were exposed to Gd<sub>2</sub>O<sub>3</sub> nanoparticles in two different concentrations (0.5 mM and 2 mM). Prior to the particle addition, half of the different cell samples were also treated with 10  $\mu$ g/mL protamine sulfate (Sigma-Aldrich Corporation, St Louis, MO) to investigate whether this could increase the particle uptake in especially the Ba/F3 cells. The samples were then incubated at 37°C in 5% carbon dioxide. THP-1 cells were incubated for 2 hours, which in previous studies was sufficient for particle uptake.<sup>15</sup> Pilot studies showed that doubling the incubation time to 4 hours did not significantly increase the uptake. Ba/F3 cells are not naturally phagocytic and therefore a longer incubation time of 24 hours was used for these cells.<sup>20</sup> After incubation, the samples were transferred into Falcon tubes (BD Biosciences, Franklin Lakes, NJ) and washed twice with cell culture medium (centrifuged for 8 minutes at 1050 rpm). For T<sub>1</sub> and T<sub>2</sub> determination, cell pellets were resuspended in 0.5 mL medium. Gelatin (0.5 mL, 2%) was added to each sample and then the samples were left to harden before MRI measurements.

Since both DEG and Gd can be toxic,<sup>21</sup> viability of Gd<sub>2</sub>O<sub>3</sub> incubated Ba/F3 cells were monitored to ensure that cells were viable prior to MRI measurements. For this, the cells were stained with trypan blue and counted in a Bürker chamber (Sigma-Aldrich, St Louis, MO) directly after 24 hours, 48 hours, and 72 hours of incubation. THP-1 cells have previously been shown to tolerate treatment with these particles for an extended period of time.<sup>15</sup>

Electron microscopy was performed to visualize intracellular Gd<sub>2</sub>O<sub>3</sub> nanoparticles. Incubated cells were washed in cell culture medium and cell pellets were fixed in 2% glutaraldehyde with 0.1 M sodium cacodylate and 0.1 M sucrose, pH 7.2. After fixation, cells were rinsed in 0.15 M sodium cacodylate buffer and postfixed in 1% osmium tetroxide in 0.15 M sodium cacodylate buffer for 2 hours. After another rinse in sodium cacodylate buffer, the samples were dehydrated in 50% ethanol twice for 5 minutes and then contrasted with 2% uranyl

acetate in 50% ethanol over night. Continuing dehydration steps was 70%, 85%, and 95% ethanol for 5 minutes each and 100% ethanol for 10 minutes. Embedding was then performed in 100% ethanol and Epon 812 (Shell Chemical LP, Houston, TX) for 30 minutes and then in pure Epon 812 for 2 hours, then polymerized in 60°C for 48 hours. Ultrathin sections (60 nm) were cut with a diamond knife (DiATOME, Bienne, Switzerland) on a Reichert-Jung Ultracut E (Leica Microsystems, Wetzlar, Germany) and collected on copper grids. Sections were stained with uranyl acetate and lead citrate and examined in a JEM 1230 electron microscope (JEOL Ltd, Tokyo, Japan) at 100 kV. Photos were taken with a SC1000 ORIUS™ CCD camera using DigitalMicrograph™ software (Gatan, Inc, Pleasanton, CA).

The cell samples were analyzed by inductively coupled plasma sector field mass spectrometry (ICP-SFMS; ALS Scandinavia AB, Luleå, Sweden) to quantify the concentration of Gd in each sample after incubation and washing. From these results uptake percentages were calculated.

## MRI

The relaxation time measurements were performed with an Achieva 1.5T A-series (Philips, Amsterdam, Netherlands) MRI scanner using a head coil. The longitudinal T<sub>1</sub> relaxation times were measured with inversion recovery sequences with turbo spin echo acquisition (turbo spin echo factor 9). Echo time was 29 milliseconds, repetition time was 10 seconds, and inversion recovery delay times were 125, 300, 500, 1000, 2000, and 5000 milliseconds. The field of view was 200 mm and slice thickness 5 mm. The transverse T<sub>2</sub> relaxation times were measured with a multiecho spin echo sequence with 16 echoes at multiples of 20 milliseconds, repetition time was 1000 milliseconds. Field of view was 200 mm and slice thickness was 5 mm.

Relaxation time measurements were performed by placing Falcon test tubes containing the samples in a holder immersed in a bowl of water at 21°C  $\pm$  1°C. For data presented in the present work, two experimental sessions were performed. At each session, relaxation times in two cell types (Ba/F3 and THP-1) incubated with Gd<sub>2</sub>O<sub>3</sub> nanoparticles with low (0.5 mM) and high (2 mM) Gd concentration respectively treated and not treated with protamine sulfate were measured. This resulted in eight measurements per session. As a reference, five Gd-diethylene triamine pentacetic acid (Magnevist®; Bayer Schering Pharma AG, Berlin, Germany) samples all containing 0.1 mM Gd in water were spread out in different places in the tube holder to ensure that the measurements were stable throughout the coil.

A monoexponential least-squares fit was performed on the data to retrieve  $T_1$  and  $T_2$ . The fit was implemented in an in-house developed Interactive Data Language program (Exelis Visual Information Solutions, Boulder, CO). Statistical analysis was obtained from GraphPad Prism® version 4 (GraphPad Software, San Diego, CA).

## Results

### Particle characterization

Gd<sub>2</sub>O<sub>3</sub> nanoparticle samples synthesized through the polyol method consist (as synthesized) of different sized particles as well as a large fraction of Gd ions. Dialysis was performed to remove the ion content and thereby an ion-free nanoparticle solution was obtained. The Gd content after 24 hours of dialysis decreased from an initial concentration of 100 mM to about 10 mM, consistent with previously published data regarding dialysis.<sup>9</sup>

To obtain information about the elemental composition of the particles, X-ray photoelectron spectroscopy measurements were performed. Results of dialyzed nanoparticle samples show a pure nanomaterial with reduced amount of hydrocarbon/DEG compared with nondialyzed material. For further details, see earlier published data.<sup>6,8,15</sup> Gd<sub>2</sub>O<sub>3</sub>-DEG particles have earlier been characterized by transmission electron microscopy showing crystalline particles with an average size of about 2–5 nm.<sup>9,16</sup> In this work, crystalline particles in the same size range were obtained.

### Cell viability

The viability of Ba/F3 cells was approximately 77% before incubation with Gd<sub>2</sub>O<sub>3</sub> nanoparticles. The corresponding value for THP-1 cells was approximately 90% before treatment with particles. In a previous study,<sup>15</sup> viability results for THP-1 cells were reported; this is therefore not further addressed in this work.

After 24 hours of incubation with Gd<sub>2</sub>O<sub>3</sub> particles at 2 mM Gd concentration, the viability of Ba/F3 cells had decreased slightly (Table 1), but not significantly. Samples were also investigated with or without protamine sulfate

added, but there was no difference between these samples. After 48 hours and 72 hours of incubation the viability was principally retained. After 72 hours the viability of the sample incubated with Gd<sub>2</sub>O<sub>3</sub> nanoparticles without protamine sulfate had decreased to 68%. However, this apparent decrease was within the standard deviation of the measurement error.

### Visualization of intracellular particles

Electron microscopy images of Gd<sub>2</sub>O<sub>3</sub> incubated cells show that THP-1 cells had a large cytoplasm and cellular parts near the cell surface indicating that they stretched out in phagocytic activity (Figure 1). In addition, particle containing vesicles were visible.

Ba/F3 cells consisted of a dominating nucleus. It is shown from the extracts in Figure 2 that Gd<sub>2</sub>O<sub>3</sub> nanoparticles resided in vacuoles inside the cells as well as outside the cell membrane in some cases. The overall results from electron microscopy images suggest that THP-1 cells contain more particles in vacuoles than Ba/F3. It is shown that Ba/F3 bound particles to the cell surface (Figure 3) and in a few cases the cells had aggregated and particles were trapped in between the cells. The ability to attract particles near the cell membrane is, however, a prerequisite for cell internalization. Visual examination of the different cell samples showed more particles in protamine sulfate-treated cells. This result was also supported by the Gd content analysis by inductively coupled plasma sector field mass spectrometry.

The analysis of Gd concentration showed a mean uptake percentage of 2% in Ba/F3 cells treated with protamine sulfate. In nontreated Ba/F3 cells, the mean uptake percentage was 1% for the low concentration and 2% for the high concentration. THP-1 had higher uptake: 5% in protamine sulfate-treated cells and 3% and 4% in nontreated cells for the low and high incubation concentration, respectively. Figure 2B and D show representative parts of control cells containing no particles. In these samples there were not as many vacuoles/endosomes present indicating that the cells were not phagocytically activated.

**Table 1** Ba/F3 cells incubated in 2 mM gadolinium compared to nontreated cells

	2 mM gadolinium + protamine sulfate	2 mM gadolinium – protamine sulfate	Control + protamine sulfate	Control – protamine sulfate
24 hours of incubation	72% ± 5%	73% ± 7%	77% ± 5%	75% ± 6%
48 hours of incubation	70% ± 7%	72% ± 11%	81% ± 6%	70% ± 4%
72 hours of incubation	73% ± 3%	68% ± 5%	83% ± 7%	75% ± 7%

**Notes:** Cells were also exposed or not exposed to transfection agent protamine sulfate. Figures in the table show percentages of viable cells.



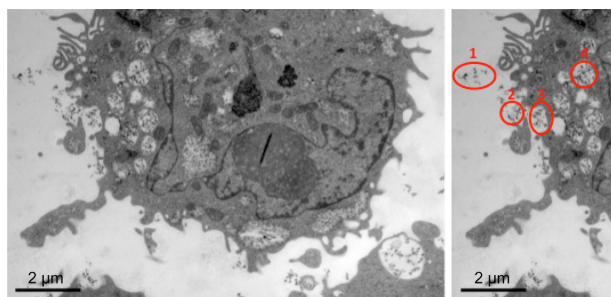


**Figure 1** Representative image of THP-1 cell treated with 2.0 mM gadolinium shows several vacuoles containing gadolinium oxide nanoparticles and invaginations at the cell surface indicating phagocytic processes (left panel). Illustration of the phagocytic process: (1) nanoparticles in the extracellular fluid, (2) nanoparticles approaching the cell surface, (3) nanoparticles at the cell surface, and (4) nanoparticles internalized in cell vacuole (right panel).

## MRI

Samples incubated with Gd<sub>2</sub>O<sub>3</sub> nanoparticles in higher Gd concentration contained higher amount of Gd and had higher relaxation rates (Figure 4). The trend was similar for both cell types. THP-1 cells treated with protamine sulfate and incubated in the higher Gd concentration had decreased relaxation rates at high Gd content (0.11 mM) compared to the expected value from the overall relaxivity trends (Table 2). In addition, relaxivity for protamine sulfate-treated THP-1 cells seemed to be lower ( $r_1 = 3.6 \text{ s}^{-1} \text{ mM}^{-1}$ ,  $r_2 = 9.6 \text{ s}^{-1} \text{ mM}^{-1}$ ) compared to the relaxivity for the other samples ( $r_1 \geq 4.5 \text{ s}^{-1} \text{ mM}^{-1}$ ,  $r_2 \geq 13.4 \text{ s}^{-1} \text{ mM}^{-1}$ ). However,  $r_1$  from the different samples were not significantly different

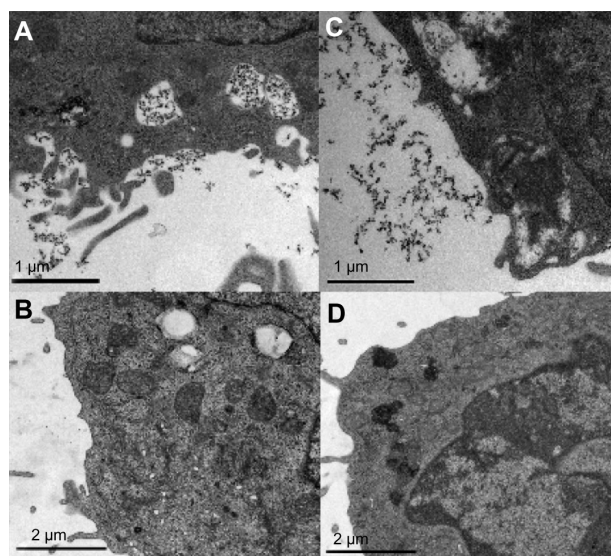


**Figure 2** Representative electron microscopy images of cells: THP-1 in (A) and (B); Ba/F3 in (C) and (D). (A) and (C) show gadolinium oxide incubated cells (treated with protamine sulfate and 2.0 mM gadolinium). Gadolinium oxide nanoparticles are visible inside vacuoles of the cell. Images (B) and (D) show control cells not treated at all. These cells do not have as many vacuoles indicating that they were not phagocytically active.

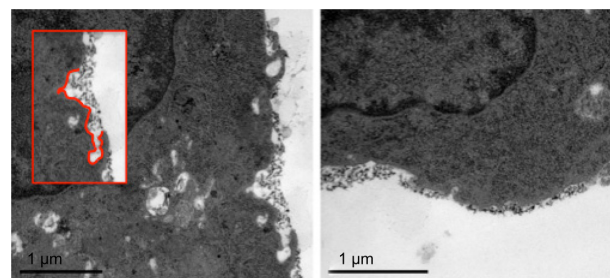


**Figure 3** Ba/F3 cells with gadolinium oxide nanoparticles on cell surface. Small endocytic invaginations (see inset) indicate a possible internalization process.

( $P = 0.08$ , pooled relaxivity across samples =  $4.4 \text{ s}^{-1} \text{ mM}^{-1}$ ), whereas  $r_2$  of the treated THP-1 cells were different from the other samples ( $P = 0.005$ ). The ratio  $r_2/r_1$  was approximately three for all cell samples.

When observing signal intensity in the top panel of Figure 5 (repetition time was 1000 milliseconds, echo time was 20 milliseconds), samples incubated with Gd<sub>2</sub>O<sub>3</sub> nanoparticles in higher Gd concentration can be seen to appear brighter. This supports the notion that high signal intensity can be obtained with intracellular Gd<sub>2</sub>O<sub>3</sub> nanoparticles. Samples incubated in 2 mM Gd with an uptake of 0.07–0.11 mM were, with these parameters, comparable in intensity to 0.1 mM Gd-diethylene triamine pentacetic acid in water. In addition, the  $T_1$  image (Figure 5, bottom panel) shows approximately the same relaxation times for samples incubated in Gd<sub>2</sub>O<sub>3</sub> nanoparticles at 2 mM Gd and the Gd-diethylene triamine pentacetic acid samples, whereas relaxation times of nanoparticle samples incubated with 0.5 mM Gd were close to the values of cell control samples.

## Discussion

### Viability and solubility uptake

Results of the Ba/F3 viability study showed that the cells were viable after incubation with Gd<sub>2</sub>O<sub>3</sub> nanoparticles and remained intact at the time for MRI measurement, which is essential for this work. Although the cells, especially Ba/F3, only partly took up the particles, they still were exposed to the Gd extracellularly, as the nanoparticles were not washed away during these observations. Taking this into account, the viability was not significantly reduced and this preserved good viability is confirmed by Faucher et al.<sup>22</sup> It is very promising that Ba/F3 cells withstand the Gd and DEG exposure to the same extent as THP-1 (previously studied in Klasson et al.<sup>15</sup> However, toxicology investigations of the Gd<sub>2</sub>O<sub>3</sub> nanoparticles need more thorough viability studies and long term biological effects need to be evaluated. In addition, it has to be remembered that before considering

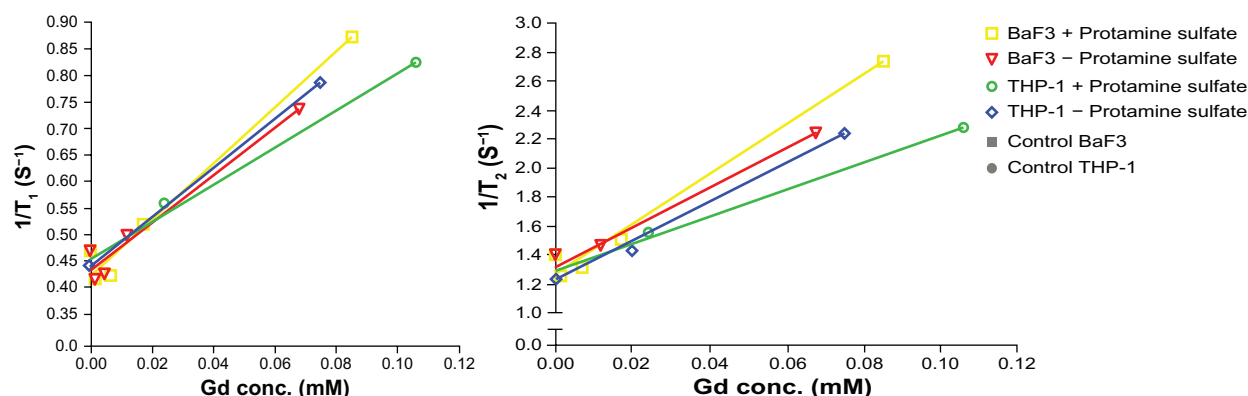


**Figure 4** Relaxation of gadolinium oxide nanoparticles in THP-1 and Ba/F3 cells. Samples were either treated with protamine sulfate or not and the cells were incubated with gadolinium oxide nanoparticles in two different gadolinium concentrations for each sample (0.5 mM or 2.0 mM).

**Abbreviations:** conc, concentration; Gd, gadolinium.

in vivo studies of the particles used as a regular contrast agent, other cappings have to be considered, hence gaining a stable, tolerable contrast agent.

As expected, Gd<sub>2</sub>O<sub>3</sub> nanoparticles were shown to be intracellularly located in THP-1 cells as well as in Ba/F3 cells. In the microscopy images, protamine sulfate effect on both Ba/F3 and THP-1 cells was observed, however not to any great extent. Higher particle content was observed in vacuoles in protamine sulfate-treated Ba/F3 compared to untreated Ba/F3 cells. THP-1 cells had high particle uptake in both protamine sulfate-treated as well as untreated cells. Because THP-1 is a naturally phagocytic cell type, this cell line is not dependent on a transfection agent for uptake. It should also be taken into account that THP-1 cells were only incubated for 2 hours, which is believed to be sufficient at regular conditions. It could, however, be beneficial to exceed that incubation time allowing the cells to interact with the transfection agent and particle solution for a longer period of time.

As previously mentioned, lower uptake was observed in endosomes and vacuoles in Ba/F3 cells than in THP-1 cells. In the electron microscopy images, extracellular Gd<sub>2</sub>O<sub>3</sub>

nanoparticles were noted near the cell membrane (Figure 3) and particles stuck in between cells. It is therefore probable that some of the measured Gd was not intracellular, but attached to the cell surface or located in between aggregated cell complexes. Another theory is that some of the intracellular particles could be located in the cytosol of the cells and therefore not clearly visible in the electron microscopy images.

In Ba/F3 cells, the low uptake was expected since these cells are not naturally phagocytic. However, lower uptake in THP-1 cells was observed in this work compared to a

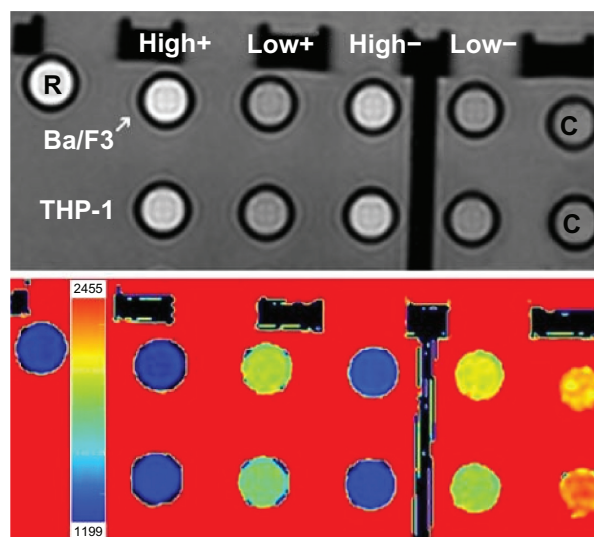


**Figure 5** Upper panel shows signal intensity of incubated cell samples (repetition time = 1000 milliseconds, echo time = 20 milliseconds). The first row is Ba/F3 and the second row is THP-1. Columns labeled "high" are treated with 2.0 mM gadolinium and "low" with 0.5 mM gadolinium. Columns labeled with "+" are protamine sulfate treated and with "-" are not treated with protamine sulfate. The rightmost samples (labeled C) are cell control samples with no particles. Sample labeled R is Gd-diethylene triamine pentacetic acid reference (0.1 mM gadolinium in water). Bottom panel shows corresponding T<sub>1</sub> map, which shows different colors corresponding to different T<sub>1</sub> times.

**Table 2** Relaxivity values  $r_1$  and  $r_2$  (s<sup>-1</sup> mM<sup>-1</sup>) at 1.5 T and 21°C for Ba/F3 and THP-1 cell samples incubated with gadolinium oxide nanoparticles with or without protamine sulfate treatment

	$r_1$	$r_2$	$r_2/r_1$
Ba/F3 + protamine sulfate	5.3 ± 0.5	17.2 ± 1.3	3.2
Ba/F3 - protamine sulfate	4.5 ± 0.5	13.4 ± 1.0	3.0
THP-1 + protamine sulfate	3.6 ± 0.3	9.6 ± 0.9	2.7
THP-1 - protamine sulfate	4.7 ± 0.8	13.6 ± 1.0	2.9

**Note:** Relaxivity calculations were based on gadolinium concentration in cells after treatment.

previous study,<sup>15</sup> which indicates that higher uptake, than seen in this work, is possible. According to the literature, the particle uptake in cells varies also at approximately similar experimental conditions.<sup>15,20,23,24</sup> It is therefore concluded that different uptake might depend on the natural and biological difference in the cells in addition to different labeling methods and incubation times. To increase the internalization of particles, in particular Gd<sub>2</sub>O<sub>3</sub> nanoparticles, other transfection agents, other incubation times, and higher incubation concentrations as well as surface modification of the particles can be considered. Dextran coating could for instance be an option, especially since dextran-coated superparamagnetic iron oxide particles show high cellular labeling efficacy.<sup>25</sup> In addition, these particles are larger than the Gd<sub>2</sub>O<sub>3</sub> nanoparticles and the particle size can be the crucial parameter. Larger particles might interact easier with the cells and would be ingested faster. Also, the efficiency of membrane wrapping processes partly depends on particle size. Previous studies have observed that nanoparticles between 25–50 nm in diameters were internalized most efficiently.<sup>26</sup> This implies that it could be beneficial to increase the size of the Gd<sub>2</sub>O<sub>3</sub> nanoparticles to make them more efficient for intracellular labeling. However, magnetic and relaxation properties might not be favored if particle size is increased.

## MRI

There was no difference in  $r_1$  relaxivity between the different cell samples treated with Gd<sub>2</sub>O<sub>3</sub> nanoparticles, but for THP-1 cells, a lower  $r_2$  relaxivity was observed for protamine sulfate-treated cells. However, more samples might be needed to ensure these results. In addition, protamine sulfate-treated cells might take up more particles concentrated to fewer vacuoles/endosomes, whereas in protamine sulfate-untreated cells the uptake might be spread in more and smaller vacuoles, which could affect the relaxivity.

Gd<sub>2</sub>O<sub>3</sub> nanoparticles in this work shortened the relaxation times with higher intracellular concentration. This is visualized in Figure 5, where samples with higher concentration have higher signal intensity (top panel), and lower  $T_1$  values (bottom panel). In contrast, the sample with THP-1 cells that had internalized the highest Gd concentration (the rightmost sample in Figure 4) had a lower relaxation rate compared to what was expected from the general trend. This result is interpreted as emanating from aggregation and/or saturation in the cells. Aggregated particles lower the relaxation rate due to a decreased surface-to-bulk ratio. Since Gd in the particle cores does not directly contribute to the relaxation effect, a decreased surface-to-bulk ratio will lead to fewer

Gd ions at the surface that could interact with intracellular protons. Decreased relaxation rate could also be an effect of vacuoles that are filled to saturation with particles. Saturated vacuoles act like macroparticles and the beneficial relaxation properties of nanoparticles are lost. However, according to Faucher et al,<sup>27</sup> Gd<sub>2</sub>O<sub>3</sub> aggregated nanoparticles could still act as an efficient “positive- $T_1$ ” contrast agent at 1–3 T magnetic fields.

## Conclusion

From the microscopy study of THP-1 and Ba/F3 cells incubated with Gd<sub>2</sub>O<sub>3</sub> nanoparticles, vacuoles with visible particles were observed. Uptake in both Ba/F3 cells and THP-1 cells was increased by the transfection agent protamine sulfate. The MRI study showed that the relaxation times were shortened with increasing particle concentration and Gd<sub>2</sub>O<sub>3</sub> nanoparticles are promising as a positive intracellular MRI contrast agent. For further studies on cell labeling, the particles need to be improved regarding capping stabilizing the particles from degradation as well as from aggregation. In addition, cell internalization, especially in cells not normally phagocytic, needs to be enhanced by modifying transfection methods and agents or optimizing incubation time. With these improvements it is possible to obtain an intracellular contrast agent generating positive contrast that could be used in pure stem cells and could contribute to the monitoring of stem cell migration.

## Acknowledgments

We thank Bengt-Arne Fredriksson (Core Facility, Health Faculty, Linköping University) for help with electron microscopy images of cells. Ann-Charlotte Bergh, Pia Druid, and Anders Rosén (Department of Clinical and Experimental Medicine, Health Faculty, Linköping University) are acknowledged for housing cell cultures and assistance in the laboratories.

Swedish Research Council (621-2007-3810, 621-2009-5148 and 521-2009-3423) is acknowledged for funding as well as VINNOVA (2009-00194) and the Center in Nanoscience and Technology at LiTH (CeNano) (2009–2010).

## Disclosure

The authors report no conflicts of interest in this work.

## References

1. Raymond KN, Pierre VC. Next generation, high relaxivity gadolinium MRI agents. *Bioconjug Chem*. 2005;16(1):3–8.
2. Rofsky NM, Sherry AD, Lenkinski RE. Nephrogenic systemic fibrosis: a chemical perspective. *Radiology*. 2008;247(3):608–612.



3. Prince MR, Zhang HL, Roditi GH, Leiner T, Kucharczyk W. Risk factors for NSF: a literature review. *J Magn Reson Imaging*. 2009;30(6):1298–1308.
4. Aime S, Caravan P. Biodistribution of gadolinium-based contrast agents, including gadolinium deposition. *J Magn Reson Imaging*. 2009;30(6):1259–1267.
5. Wertman R, Altun A, Martin DR, et al. Risk of nephrogenic systemic fibrosis: evaluation of gadolinium chelate contrast agents at four American universities. *Radiology*. 2008;248(3):799–806.
6. Ahrén M, Selegård L, Klasson A, et al. Synthesis and characterization of PEGylated  $Gd_2O_3$  nanoparticles for MRI contrast enhancement. *Langmuir*. 2010;26(8):5753–5762.
7. Bridot JL, Faure AC, Laurent S, et al. Hybrid gadolinium oxide nanoparticles: multimodal contrast agents for in vivo imaging. *J Am Chem Soc*. 2007;129(16):5076–5084.
8. Engström M, Klasson A, Pedersen H, Vahlberg C, Käll PO, Uvdal K. High proton relaxivity for gadolinium oxide nanoparticles. *MAGMA*. 2006;19(4):180–186.
9. Fortin MA, Petoral RM Jr, Söderlind F, et al. Polyethylene glycol-covered ultra-small  $Gd_2O_3$  nanoparticles for positive contrast at 1.5T magnetic resonance clinical scanning. *Nanotechnology*. 2007;18(39):395501.
10. Weissleder R, Cheng HC, Bogdanova A, Bogdanov A Jr. Magnetically labeled cells can be detected by MR imaging. *J Magn Reson Imaging*. 1997;7(1):258–263.
11. Bonde J, Hess DA, Nolta JA. Recent advances in hematopoietic stem cell biology. *Curr Opin Hematol*. 2004;11(6):392–398.
12. Janic B, Iskander AS, Rad AM, Soltanian-Zadeh H, Arbab AS. Effects of ferumoxides-protamine sulfate labeling on immunomodulatory characteristics of macrophage-like THP-1 cells. *PLoS One*. 2008;3(6):e2499.
13. Küstermann E, Himmelreich U, Kandal K, et al. Efficient stem cell labeling for MRI studies. *Contrast Media Mol Imaging*. 2008;3(1):27–37.
14. Rad AM, Arbab AS, Iskander AS, Jiang Q, Soltanian-Zadeh H. Quantification of superparamagnetic iron oxide (SPIO)-labeled cells using MRI. *J Magn Reson Imaging*. 2007;26(2):366–374.
15. Klasson A, Ahrén M, Hellqvist E, et al. Positive MRI contrast enhancement in THP-1 cells with  $Gd_2O_3$  nanoparticles. *Contrast Media Mol Imaging*. 2008;3(3):106–111.
16. Bazzi R, Flores-Gonzalez MA, Louis C, et al. Synthesis and luminescent properties of sub-5-nm lanthanide oxide nanoparticles. *J Lumin*. 2003;102–103:445–450.
17. Söderlind F, Pedersen H, Petoral RM Jr, Käll PO, Uvdal K. Synthesis and characterization of  $Gd_2O_3$  nanocrystals functionalized by organic acids. *J Colloid Interface Sci*. 2005;288(1):140–148.
18. Palacios R, Henson G, Steinmetz M, McKearn JP. Interleukin-3 supports growth of mouse pre-B-cell clones in vitro. *Nature*. 1984;309(5964):126–131.
19. Tsuchiya S, Yamabe M, Yamaguchi Y, Kobayashi Y, Konno T, Tada K. Establishment and characterization of a human acute monocytic leukemia cell line (THP-1 cells). *Int J Cancer*. 1980;26(2):171–176.
20. Daldrop-Link HE, Rudelius M, Oostendorp RA, et al. Targeting of hematopoietic progenitor cells with MR contrast agents. *Radiology*. 2003;228(3):760–767.
21. Palasz A, Czekaj P. Toxicological and cytophysiological aspects of lanthanide actions. *Acta Biochim Pol*. 2000;47(4):1107–1114.
22. Faucher L, Guay-Bégin AA, Lagueux J, Côté MF, Petitclerc E, Fortin MA. Ultra-small gadolinium oxide nanoparticles to image brain cancer cells in vivo with MRI. *Contrast Media Mol Imaging*. 2011;6(4):209–218.
23. Wilhelm C, Gazeau F, Roger J, Pons JN, Bacri JC. Interaction of anionic superparamagnetic nanoparticles with cells: kinetic analyses of membrane adsorption and subsequent internalization. *Langmuir*. 2002;18(21):8148–8155.
24. Maxwell DJ, Bonde J, Hess DA, et al. Fluorophore conjugated iron oxide nanoparticle labeling and analysis of engrafting human hematopoietic stem cells. *Stem Cells*. 2008;26(2):517–524.
25. Matuszewski L, Persigehl T, Wall A, et al. Cell tagging with clinically approved iron oxides: feasibility and effect of lipofection, particle size, and surface coating on labeling efficiency. *Radiology*. 2005;235(1):155–161.
26. Vance D, Martin J, Patke S, Kane RS. The design of polyvalent scaffolds for targeted delivery. *Adv Drug Deliv Rev*. 2009;61(11):931–939.
27. Faucher L, Gossuin Y, Hocq A, Fortin MA. Impact of agglomeration on the relaxometric properties of paramagnetic ultra-small gadolinium oxide nanoparticles. *Nanotechnology*. 2011;22(29):295103.

## International Journal of Nanomedicine

### Publish your work in this journal

The International Journal of Nanomedicine is an international, peer-reviewed journal focusing on the application of nanotechnology in diagnostics, therapeutics, and drug delivery systems throughout the biomedical field. This journal is indexed on PubMed Central, MedLine, CAS, SciSearch®, Current Contents®/Clinical Medicine,

Submit your manuscript here: <http://www.dovepress.com/international-journal-of-nanomedicine-journal>

Dovepress

Journal Citation Reports/Science Edition, EMBase, Scopus and the Elsevier Bibliographic databases. The manuscript management system is completely online and includes a very quick and fair peer-review system, which is all easy to use. Visit <http://www.dovepress.com/testimonials.php> to read real quotes from published authors.